IEEE Access
Multidisciplinary | Rapid Review | Open Access Journal

Received October 26, 2020, accepted November 8, 2020, date of publication November 16, 2020,
date of current version November 25, 2020.

Digital Object Identifier 10.1109/ACCESS.2020.3037753

PWC-PON: An Energy-Efficient Low-Latency DBA Scheme for Time Division Multiplexed Passive Optical Networks

MIN ZHU[1,2], (Member, IEEE), JIAHUA GU[1,2], AND GUIXIN LI[3]
[1]National Mobile Communication Research Laboratory, Southeast University, Nanjing 210096, China
[2]Purple Mountain Laboratories, Nanjing 211111, China
[3]School of Electronic Science and Engineering, Southeast University, Nanjing 210096, China

Corresponding author: Min Zhu (minzhu@seu.edu.cn)

This work was supported in part by the National Natural Science Foundation of China (NSFC) under Grant 61771134, and in part by the Transformation Program of Scientific and Technological Achievements of Jiangsu Province under Grant BA2019026.

ABSTRACT Reducing network energy consumption and offering low-latency service quality have been the pursued goals in broadband passive optical networks (PONs). To realize these goals, energy-efficient dynamic bandwidth allocation (DBA) has been extensively studied. Nevertheless, few of these DBA schemes can effectively support low-latency and low-energy requirements, simultaneously. For these existing DBA schemes, the adopted energy-saving methods by sleeping some network elements would not handle the mismatch between the upstream and downstream bandwidth required by an optical network unit (ONU), which brings in a longer active window for each ONU and thus larger packet latencies. In this paper, an energy-efficient low-latency DBA scheme is proposed based on a novel pairwise combination (PWC) method. The essence of the PWC method is to compact the polling cycle length as much as possible by dynamically paring any two ONUs in complementary ways, which in turn also improves latency performance of data packets (i.e., quality of service (QoS)). Moreover, we introduce a multiple-state energy-saving mode into the proposed DBA scheme to reduce the PON energy consumption, with the consideration of both the upstream (US) and downstream (DS) transmissions. We establish an energy saving model for the proposed PWC-PON compared with the PONs with the existing DBA schemes, and also present a comprehensive M/G/1 queuing analysis with modification for the data latency performance. Extensive theoretical analysis and simulation results show that the proposed PWC-PON can reduce US and DS latency by 50% compared with the existing Gate Service (GS)-based DBA scheme. The energy saving efficiency is up to 3.5% higher than the benchmark when the US traffic load is light. It suggests that our PWC-based DBA scheme cannot only reduce the energy consumption, but also reduce the packet latency for PON system.

INDEX TERMS Energy-saving, passive optical network (PON), pairwise combination passive optical network (PWC-PON), dynamic bandwidth allocation (DBA), data latency analysis, M/G/1 queuing.

I. INTRODUCTION

The arrival of Information Age has led to wide deployment of network infrastructures, where a plenty of optical and electronic elements are necessary. These network elements require a considerable amount of energy, which accounts for a large slice of the total operational costs of construction. Thus, the network energy consumption has become a serious issue that may in turn affect the further development of networks. As reported [1], the access network segments account for the highest proportion of the energy consumption, compared to other network segments. Hence, for sustainable development, it is more and more urgent for network operators to construct an energy-efficient access network.

Time division multiplexed passive optical network (TDM- PON) such as Ethernet PON (EPON) and Gigabit PON (GPON) is a promising solution for providing broadband access services to end devices/users and have being deployed worldwide [2]. In a TDM-PON, an optical line terminal (OLT) located in central office (CO) of the network

The associate editor coordinating the review of this manuscript and approving it for publication was Tianhua Xu.

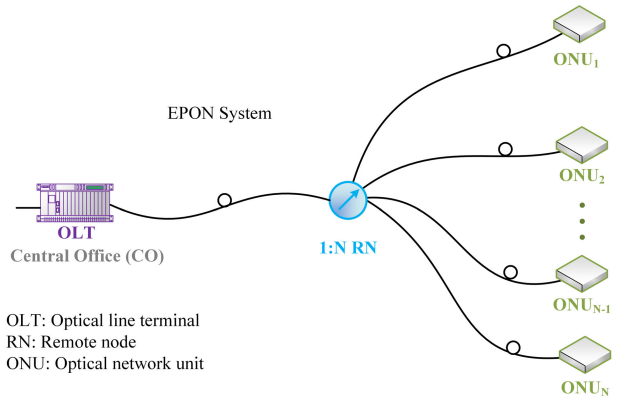

FIGURE 1. An EPON based optical access network.

operator connects customer-side multiple optical network units (ONUs) through tree-topology fiber links, as shown in Fig. 1. A passive splitter is placed at a remote node (RN). In the upstream (US) from ONUs to OLT, the bandwidth of the fiber link is shared within all connected ONUs in a TDM way. Each ONU sends its US frame during a dedicated time slot assigned by the OLT, which uses dynamic bandwidth allocation (DBA) scheme to decide each ONU's dedicated US transmission slot. From OLT to ONUs, the downstream (DS) frames are broadcast to all ONUs and each ONU filters out its belonging DS frames (e.g., using a logical link identifier in EPON).

Although the TDM-PON is the most energy-efficient access technology, compared with other PON technologies [1], [2], the energy consumption in TDM-PONs still need to be reduced due to a large amount of the ONUs used in access networks. Some previous works to improve the ONU energy efficiency has been reported by introducing a sleep-mode based state transition mechanism into the DBA scheme for TDM-PONs. Since the traffic of ONUs is rather bursty and varies dynamically, putting idle ONUs into sleep mode can significantly reduce ONU energy consumption [3], [4]. In [5], authors tried to find the optimal value of the sleep period in the cycle sleep mode to realize a performance tradeoff between power consumption and state transition delay in ONU. In [6], a watchful sleep mode is designed, which unifies both Doze and Cyclic Sleep modes to further reduce ONU energy consumption. However, these schemes can only be applied to the US traffic, while any DS traffic is not considered. It means that the DS channels are always in the active state. Therefore, the two schemes cannot improve the energy efficiency of a realistic PON to the greatest extent. The literatures [7], [8] considered both the US and DS traffic, and proposed two policies with different priorities: US Centric Scheduling (UCS) and DS Centric Scheduling (DCS). Both schemes allocate the transmission time slot for each ONU only depend on either of US and DS traffic, and the relationship between the US and DS traffic is ignored. Recently, in [9], a novel energy-efficient dynamic bandwidth allocation policy named Gate Service (GS) has been proposed. In the scheme, the ONU is always allocated a bandwidth (i.e., time slot) equal to the maximum value of its requested US- and DS-bandwidth, as shown in Fig. 2. However, the GS scheme may result in the waste of the bandwidth and energy resources, due to the significant mismatch between the requested US- and DS-bandwidth. Another disadvantage worth mentioning in the above schemes is that the ONU polling sequence is always fixed. It is lack of the flexibility of allocating bandwidth and causes longer polling cycles.

One other issue of concern is the traffic latency performance in PONs, which has great impact on Quality of Service (QoS). It cannot completely rely on upgrading network equipment to improve latency, but must adopt some advanced DBA algorithms [10]–[12]. In [10], the authors proposed a scheme named low-latency polling (LLP), which decouples the REPORT frame from US data transmissions. Meanwhile, the LLP scheme schedules the REPORT frame so that it arrives at the OLT before the upstream data are scheduled to be transmitted. The authors in [11] designed a QoS-guaranteed DBA scheme for a unique OFDMA-PON architecture. Such scheme fully utilizes the frames in a statistical method. In [12], authors proposed an enhanced QoS-enabled DBA mechanism, which calculates a set of complementary bandwidth amounts to assign to the ONUs during the idle time. The authors in [13] introduced the sleep mode into the DBA scheme in PON, and establish a mathematical model for average packet delay. In [14], authors proposed a novel DBA scheme to converge mobile fronthaul (MFH) and Internet of Things (IoT) networks on a single TDM-PON. It simultaneously provides low-latency transmission, bandwidth guarantee and an auto-discovery process. Authors in [15] proposed a dynamic bandwidth and wavelength allocation (DBWA) algorithm that uses bin-packing approach to improve energy efficiency and delay performance of time and wavelength division multiplexed PONs (TWDM-PONs). In [16], authors proposed a novel medium access control (MAC) protocol for 10 Gigabit-capable PONs (XGPONs), which jointly allocates bandwidth and wavelength resources to transmission container (T-CONT) groups to fulfill QoS requirements. It significantly increases throughput and reduces end-to-end packet delay. However, these schemes mentioned above only consider the US transmission, while the DS traffic is ignored.

In our preliminary work [17], an energy-efficient low latency DBA scheme was introduced based on a pairwise combination (PWC) method, and simulation investigation is given out. In the paper, we formulate a comprehensive M/G/1 queuing analysis with modification for the data latency performance for the proposed PWC-based DBA (i.e., PWC-PON) scheme in PONs. The PWC method pairs any two ONUs in complementary ways due to the fact that the mismatch between both the US and DS transmission. Theoretical analysis and extensive simulation are carried out. Compared with the existing energy-efficient GS-based DBA scheme, results show that the proposed PWC-PON scheme

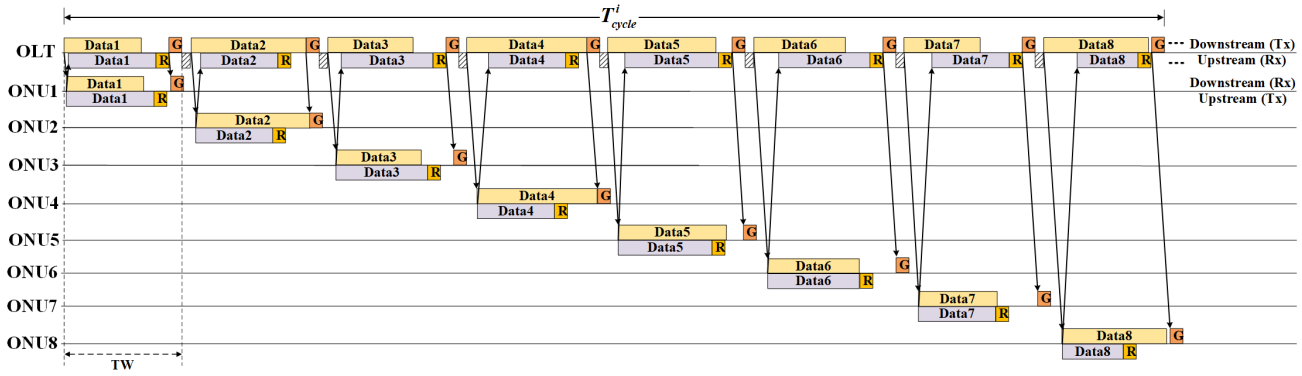

FIGURE 2. Traffic flow of the existing GS-based DBA scheme for a PON segment [9].

can not only greatly reduce traffic latency by compacting the polling cycle length, but also effectively improve the ONU energy efficiency through multiple-state energy-saving mode.

Note that the EPON standard has been selected to carry out the research in this paper. Since the proposed PWC-based DBA scheme mainly focus on the dynamic bandwidth resource allocation for TDM-PON, it can be easily adapted to other PON technologies such as GPON and 10G-EPON.

The remainder of this paper is organized as follow. Section II presents a detailed theoretical analysis of our proposed PWC-PON scheme. Section III shows the energy saving model. The mean packet delay is analyzed in Section VI. Thorough numerical analyses are performed in Section V. Finally, a conclusion is discussed in Section VI.

II. PRINCIPLES AND THEORETICAL ANALYSIS

In this study, an EPON-based access network with its typical tree-and-branch topology consists of N ONUs and an OLT is shown in Fig. 1. Generally, the fiber length between the ONUs and the OLT ranges from 10 km to 100 km [9]. The OLT manages both the DS and US transmissions of all ONUs and schedules the network resources. For the conventional PON with fixed polling sequence, in the DS direction, the OLT broadcasts the GATE messages and DS data to all ONUs, and allocates their US bandwidth in terms of the time window (TW) according to the ONUs' REPORT messages. Each ONU receives their DS data using a logical link identifier (LLID) in the EPON. In the US direction, ONUs transmit their US data to the OLT one by one in a TDM way.

Fig. 2 illustrates the traffic flow of the existing GS-based DBA scheme. In the figure, the yellow block is the US data that ONU sends to OLT, and purple block is the DS data that OLT sends to ONU. In each TW, an ONU sends US data to OLT and receives DS data from OLT. There are three arrows in each TW, which indicates the DS data transmission, US data transmission and GATE message transmission in turn. The overall aim of this scheme is to design the optical access network to work in a TDM way in order to turn the ONU into sleep state for saving energy. Every ONU transmits and receives the US/DS data within its transmission time window (TW), which is equal to the maximum value of the US- and DS-bandwidth. Outside the TW, the corresponding ONU enters into the sleep state.

In Fig. 3, a traffic flow of the proposed PWC-based DBA scheme is shown. For the purpose of simplicity and clarity, only $N = 8$ ONUs are drawn. They are partitioned into two groups ($\alpha = 2$). In each group, four ONUs will be made pairs respectively by using the proposed PWC method. Since this novel scheme is compatible with the existing Multi-Point Control Protocol (MPCP) in TDM-PON, the polling sequence scheduling messages is updated to each ONU via GATE/ REPORT frame [18].

A. PWC-PON SCHEME

Figure 4 illustrates the proposed PWC-PON scheme executed at the ONU and the OLT.

After the initialization procedure, the ONU operations are performed in the following main three steps:

Step 1: Once receiving the GATE message from the OLT, the ONU parses the message and obtains the TWs and its polling sequence, which includes the start time and the duration time of the US- and DS-TWs, respectively.

Step 2: Once the ONU local clock *onu_clock* reaches the designated start time *Rx_start* and *Tx_start*, the ONU is waked up and starts its DS-TW and US-TW, respectively. If the DS-TW starts first (and the US-TW not started yet), the ONU is in the listen state for receiving DS data. Otherwise, when the US-TW opens, the ONU enters into the active state to send its US data up to the size of the granted US-TW. Meanwhile, the ONU keeps receiving new data packets from its end users and storing these data in its buffer. After finishing the US transmission, the ONU generates the REPORT message for the required US bandwidth in the next polling cycle, and then sends out the REPORT message.

Step 3: Afterwards, if the ONU is still receiving the DS data, the ONU can switch its state from the active into the listen mode; otherwise, it means that the DS transmission finishes too. Hence the ONU can shut down its transceiver

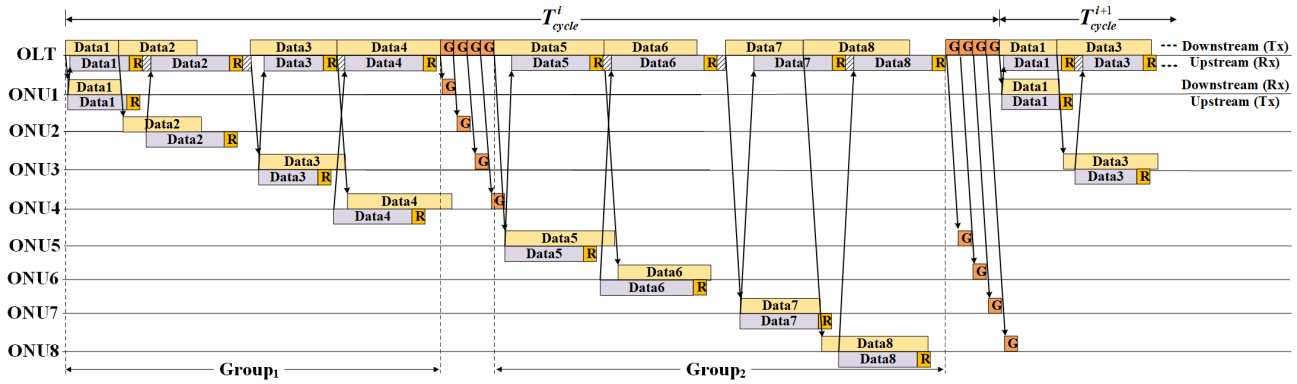

FIGURE 3. Traffic flow of the proposed PWC-based DBA scheme with two groups ($\alpha = 2$).

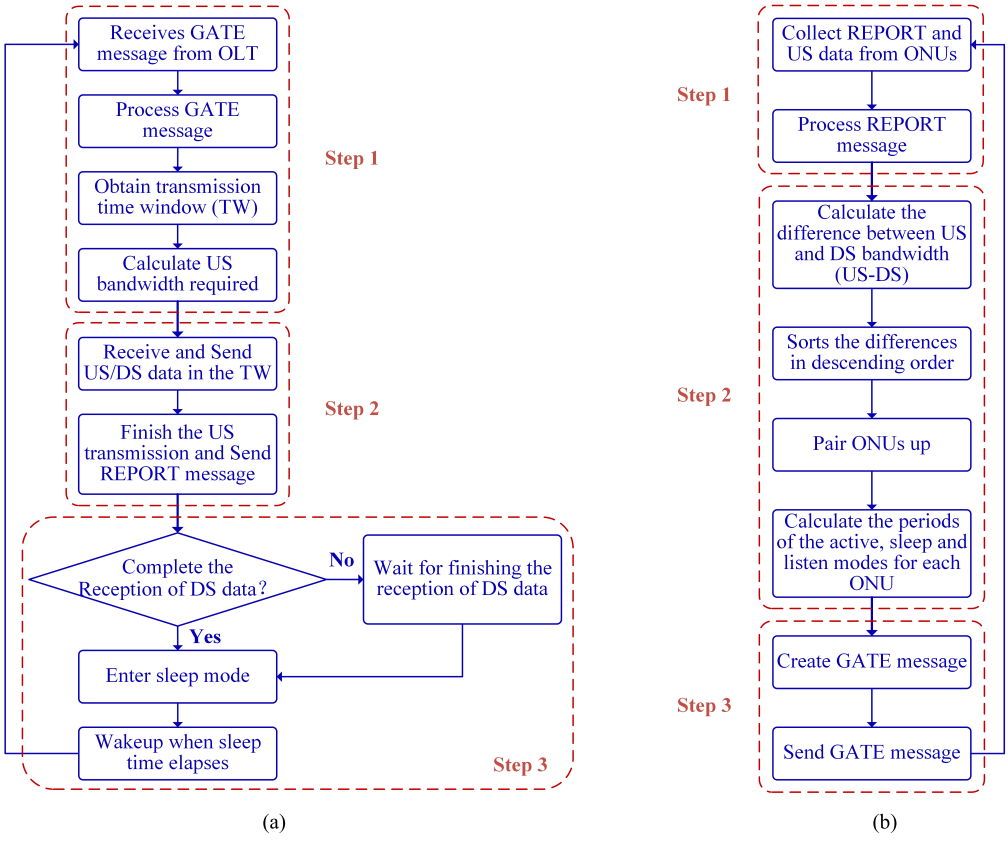

FIGURE 4. Flow chart of the proposed PWC-PON scheme performed at (a) the ONU and (b) the OLT.

to enter into sleep state for energy-saving until it is waked up in the next polling cycle.

In the OLT side, as shown in fig. 4 (b), the PWC-based DBA scheduling operations are done in the following three steps, which can be referred to Fig. 5.

Step 1: The OLT collects the US data and REPORT messages from all the ONUs that are in the same group. And it processes the REPORT messages and extracts their required US bandwidths.

Step 2: According to the known DS bandwidth requirement, which is OLT local information, the difference value between US- and DS-bandwidth can be calculated for each ONU. As shown in the half bottom of Fig. 5, the OLT can sort these difference values in descending order. Then the head and the tail of the ordering list are paired off to offset their US&DS mismatch to each other. Thus, all the ONUs in the PON are paired off using the proposed PWC method.

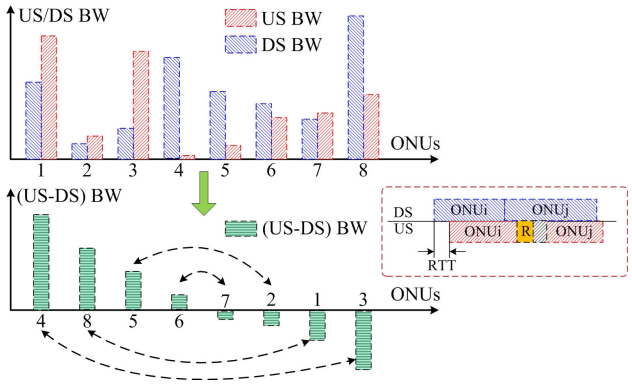

FIGURE 5. PWC operation principle in the OLT.

Step 3: According the above combination results, the OLT generates the GATE messages and sends to all ONUs that are in the same group.

B. GRANTED TW CALCULATION FOR DIFFERENT DBA SCHEMES

In the proposed PWC-PON scheme, the shared TW T_{len} for any two combined ONUs is calculated in (1). For example, as shown in Fig. 3, the ONU1 and ONU2 have been combined together.

$$T_{len}^{PWC} = \max\{B_{d1} + B_{d2} + T_g, RTT + B_{u1} + B_{u2} + 2T_{msg} + T_g\} \quad (1)$$

where RTT is round-trip time, T_{msg} and T_g are MPCP message time and guard time, respectively, and B_{d1} and B_{u1} are the required DS- and US- bandwidth of the ONU1 in this combination; while the B_{d2} and B_{u2} refer to the required DS- and US-bandwidth of the ONU2.

However, in the existing GS-based DBA scheme as shown in Fig. 2, the corresponding TW for the successive two ONUs can be computed in the following (2).

$$T_{len}^{GS} = \max\{B_{d1}, RTT + B_{u1} + T_{msg}\} + T_{msg} + \max\{B_{d2}, RTT + B_{u2} + T_{msg}\} + T_{msg} + T_g \quad (2)$$

III. ENERGY CONSUMPTION MODEL

In this section, the energy consumption model of EPON is established. The considerable energy efficiency gain arising from the proposed PWC-PON scheme over the two existing benchmark DBA schemes is analyzed. The first benchmark is the well-known interleaved polling with adaptive cycle time (IPACT) scheme without any energy-saving consideration [18]. By contrast, the energy-saving efficiency η^{PWC} of the PWC-PON is defined for an ONU within a cycle time as follow:

$$\eta^{PWC} = \frac{E^{IPACT} - E^{PWC}}{E^{IPACT}} = 1 - \frac{E^{PWC}}{E^{IPACT}} \quad (3)$$

where E^{IPACT} is the average energy consumption of an ONU in one scheduling period T_c, when the EPON is always active. In the case the PWC-PON scheme is enabled, the E^{PWC} denotes the ONU average energy consumption during a T_c. The calculation of the E^{IPACT} is given by:

$$E^{IPACT} = T_c \times P_{active} \quad (4)$$

where parameter P_{active} refers to the ONU power consumption in the active state. The E^{PWC} is computed as follow:

$$E^{PWC} = T_{active}^{PWC} \times P_{active} + T_{listen}^{PWC} \times P_{listen} + T_{sleep}^{PWC} \times P_{sleep} \quad (5)$$

where parameters T_{active}^{PWC}, T_{listen}^{PWC}, and T_{sleep}^{PWC} refer to the duration time of the active, listen, and sleep modes during the scheduling period, respectively. The descriptions and considered values of the P_{active}, P_{listen} and P_{sleep} are provided in Table 1.

TABLE 1. Values of evaluation parameters.

Notation	Description	Value	Source
N	Number of ONUs in system	16 or 32 or 64	[18]
R	Line rate	1 Gbps	[18]
P_{min}	Min packet size	64 bytes	[18]
P_{max}	Max packet size	1518 bytes	[18]
B	Buffer size in ONU	1 Mbytes	[18]
T_g	Guard band time	1000 ns	[18]
T_{prop}	Propagation delay	5 ns / meter	[18]
P_{active}	ONU power consumption in active state	100%	[6]
P_{listen}	ONU power consumption in listen state	40%	[6]
P_{sleep}	ONU power consumption in sleep state	5%	[6]

The scheduling time T_c^{PWC} for the PWC-PON scheme is computed as the sum of T_{active}^{PWC}, T_{listen}^{PWC}, and T_{sleep}^{PWC}, as (6).

$$T_c^{PWC} = T_{active}^{PWC} + T_{listen}^{PWC} + T_{sleep}^{PWC} \quad (6)$$

During the scheduling period T_c^{PWC}, T_{active}^{PWC} is defined to be the duration time of transmitting US traffic to the OLT, while T_{listen}^{PWC} is the duration time just for receiving DS traffic. The rest time in the period T_c^{PWC} is considered as T_{sleep}^{PWC}.

For the second benchmark GS-based DBA scheme, which adopts energy-saving policy, the ONU can be waked up only within its TW to transmit/receive the US and the DS data, simultaneously. Outside the allocated TW, the ONU will be switched into the sleep state for energy-saving. Similarly, the energy-saving efficiency η^{GS} for the GS-based DBA scheme is calculated in the same scheduling period $T_c^{PWC} = T_c^{GS}$ as follow:

$$\eta^{GS} = \frac{E^{IPACT} - E^{GS}}{E^{IPACT}} \quad (7)$$

where the E^{GS} and T_c^{GS} can be defined as:

$$E^{GS} = T_{active}^{GS} \times P_{active} + T_{sleep}^{GS} \times P_{sleep} \quad (8)$$

$$T_c^{GS} = T_{active}^{GS} + T_{sleep}^{GS} \quad (9)$$

IV. ANALYSIS OF THE MEAN PACKET DELAY

In this section, we provide a detailed analysis of the delay of PWC-based DBA scheme for US and DS traffic. The packet delay is defined as the total time, which is a packet spends in the PON from the time that it is generated until it is transmitted at the OLT and vice versa. In recent years, a lot of researches about delay performance for PON have been done by experts worldwide. What's more, different kinds of delay models with or without sleeping mechanisms of ONU are proposed [19]–[21]. However, those delay analysis models mentioned above did not take a mismatch between the bandwidth requirement of US and DS into consideration.

In the PWC scheme, we analyze the average US and DS traffic delay by adopting an M/G/1 queuing model with vacation queuing model, which has been modified to fit with the scheduling system [21]. For the sake of analysis, we assume that the maximum allowable $TW^{\max}$, which is assigned to the ONU by the OLT, can actually go to infinity. For this reason, not only the upstream traffic transmissions but also the downstream traffic transmissions can be granted at least the required bandwidth, in other words, the size of each ONU's TW is the maximum between the required US and DS bandwidth.

The EPON system, which is adopted to analyze the average traffic delay, has N ONUs and an OLT. It is assumed that every ONU is equipped with a packet buffer, and this buffer can store the data quickly. In addition, every buffer's capacity is assumed to be large enough, and this scheduling system does not have any packet loss even though the traffic load ρ is high.

US and DS frames are generated by using self-similar traffic model and the arrival rates are defined respectively as λ_u and λ_d. $\overline{X}_u$ and $\overline{X}_d$ are viewed as the average time needed to serve the US frame and DS frame, while $\overline{X_u^2}$ and $\overline{X_d^2}$ are the secondary moment. The first and second moments of US reservation time are denoted by $\overline{V}_u$ and $\overline{V_u^2}$, and the first and second moments of DS reservation time are denoted by $\overline{V}_d$ and $\overline{V_d^2}$. Aggregate upstream and downstream traffic loads are viewed as $\rho_u = \lambda_u \overline{X}_u$ and $\rho_d = \lambda_d \overline{X}_d$, respectively. Table 2 lists the relevant parameters in the mean packet delay analysis.

A. MEAN US FRAME DELAY

During the transmission window, the OLT receives US data and REPORT messages from all the ONUs that are in the same group. Afterwards, the OLT goes on "vacation" and sends GATE frames to all ONUs that are in the same group. As can be seen from Fig. 6, every cycle length is made up of several parts, and they are N data intervals, N reservation intervals, $N/2$ Round-Trip Time (RTT) intervals, and 1 GATE interval ("vacation" interval).

In PWC scheme, reservation time V_u is defined as the sum of GATE/REPORT message time T_{msg} and data guard timeT_g. Consequently, the value of V_u is equal to $T_{msg} + T_g$, which is a constant.

TABLE 2. Parameters in the mean packet delay analysis.

Notation	Description
$\overline{X}$	First moment of packet service time
$\overline{X^2}$	Second moment of packet service time
λ	Packet arrival rate
ρ	Network traffic load
V	Reservation time (the sum of REPORT message time and data guard time)
S	RTT interval time
G	GATE frame interval time
ξ	Steady state probability of RTT intervals
k	Steady state probability of GATE frame intervals
R	Residual delay
W	Queuing delay
Y	Reservation-and-vacation delay
Q	Service delay

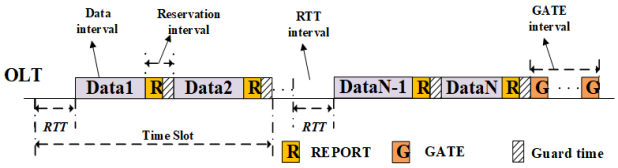

FIGURE 6. M/G/1 queueing model of US scheduling.

The mean US packet latency $\overline{W}_u$ is composed of three parts: the residual delay $\overline{R}_u$, the service delay $\overline{Q}_u$, and the reservation-and-vacation delay $\overline{Y}_u$. It can be written as:

$$\overline{W}_u = \overline{R}_u + \overline{Q_u} + \overline{Y}_u \tag{10}$$

We use the following definitions for the three parameters:

The residual delay $\overline{R}_u$ is equal to the residual time that the system needed to finish the on-going data interval or the RTT interval or the GATE interval.

The service delay $\overline{Q}_u$ is equal to the time for sending all the data packages to the OLT, and these packages arrived at the data buffer before this particular frame.

The reservation-and-vacation delay $\overline{Y}_u$ is equal to the total time of reservation intervals, RTT intervals, and GATE frame intervals.

According to Little's Theorem, the service delay $\overline{Q}_u$ can be expressed as follows:

$$\overline{Q}_u = \rho_u \times \overline{W_u} \tag{11}$$

Hence, $\overline{W}_u$ can be computed as:

$$\overline{W}_u = \overline{R}_u + \rho_u \times \overline{W_u} + \overline{Y}_u = \frac{1}{1-\rho_u}(\overline{R}_u + \overline{Y_u}) \tag{12}$$

Lemma 1: The residual delay $\overline{R}_u$ of upstream traffic delay in PWC scheme can be defined as:

$$\overline{R}_u = \frac{\rho_u \overline{X_u^2}}{2\overline{X_u}} + \frac{\left(2NV_u^2 + NS_u^2 + 2G_u^2\right)(1-\rho_u)}{2(NV_u + (N/2)S_u + G_u)} \tag{13}$$

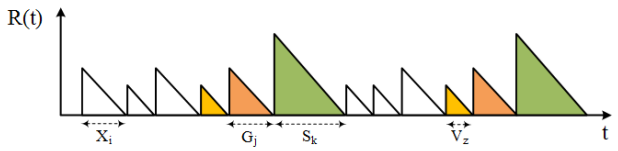

FIGURE 7. Residual delay component.

Proof: The residual delay is derived from the graphical argument, as shown in Fig. 7, and the analytical approach is similar to that in [21]. $\overline{R}_u$ can be written as:

$$\begin{aligned}\overline{R}_u &= \lim_{t\to\infty}\frac{1}{t}\int_0^t R(\tau)d\tau = R_1+R_2+R_3+R_4\\ &= \lim_{t\to\infty}\frac{1}{t}\sum_{i=1}^{X_u(t)}\frac{X_i^2}{2}+\lim_{t\to\infty}\frac{1}{t}\sum_{i=1}^{V_u(t)}\frac{V_i^2}{2}\\ &\quad+\lim_{t\to\infty}\frac{1}{t}\sum_{i=1}^{S_u(t)}\frac{S_i^2}{2}+\lim_{t\to\infty}\frac{1}{t}\sum_{i=1}^{G_u(t)}\frac{G_i^2}{2}\end{aligned}\tag{14}$$

where $X_u(t)$, $V_u(t)$, $S_u(t)$ and $G_u(t)$ are the numbers of data packets, reservation intervals, RTT intervals and GATE intervals to time t, respectively. Moreover, X_i, V_i, S_i and G_i denote the time duration of the i^{th} data packet, reservation intervals, RTT intervals and GATE intervals. In the limit as $t\to\infty$, $X_u(t)/t$ can be viewed as the average of the departure rate λ_u, and λ_u is equal to $\rho_u/\overline{X}_u$. Hence, R_1 can be computed as follows:

$$\begin{aligned}R_1 &= \lim_{t\to\infty}\frac{1}{t}\sum_{i=1}^{X_u(t)}\frac{X_i^2}{2}=\lim_{t\to\infty}\frac{X_u(t)}{t}\frac{\sum_{i=1}^{X_u(t)}X_i^2}{2X_u(t)}\\ &= \frac{\lambda_u\overline{X_u^2}}{2}=\frac{\rho_u\overline{X_u^2}}{2\overline{X}_u}\end{aligned}\tag{15}$$

Likewise, $V_u(t)/t$ can be viewed as the average of the reservation rate, which is equal to $(1-\rho_u-\xi_u-k_u)/\overline{V}_u$. ξ_u, k_u are the steady state probability of RTT intervals and GATE frame intervals, respectively. Hence, R_2can be given by:

$$\begin{aligned}R_2 &= \lim_{t\to\infty}\frac{1}{t}\sum_{i=1}^{V_u(t)}\frac{V_i^2}{2}=\lim_{t\to\infty}\frac{V_u(t)}{t}\frac{\sum_{i=1}^{V_u(t)}V_i^2}{2V_u(t)}\\ &= \frac{(1-\rho_u-\xi_u-k_u)\overline{V_u^2}}{2\overline{V}_u}=\frac{(1-\rho_u-\xi_u-k_u)\overline{V}_u}{2}\end{aligned}\tag{16}$$

$S_u(t)/t$is defined as RTT rate, i.e., how many RTT intervals the system has in a time unit. In PWC scheme, every polling cycle only contains $N/2$ RTT intervals, when $t\to\infty$. Hence, we can write:

$$\frac{S_u(t)}{N/2}\overline{T}_c = t\tag{17}$$

and

$$\frac{S_u(t)}{t}=\frac{N}{2\overline{T}_c}\tag{18}$$

Consequently, R_3 becomes:

$$R_3=\lim_{t\to\infty}\frac{1}{t}\sum_{i=1}^{S_u(t)}\frac{S_i^2}{2}=\lim_{t\to\infty}\frac{S_u(t)}{t}\frac{\sum_{i=1}^{S_u(t)}S_i^2}{2S(t)}=\frac{N\overline{S_u^2}}{4\overline{T}_c}\tag{19}$$

In addition, S_u is defined as the duration of RTT interval, which is a constant as well as $\overline{S}_u$ and $\overline{S_u^2}$. Since the portion of RTT intervals in upstream transmission is equal to ξ_u, $N/2\times\overline{S}_u$ is derived from $\overline{T}_c\xi_u$. Finally, we can write $\overline{T}_c$ as:

$$\overline{T}_c=\frac{N\times\overline{S}_u}{2\times\xi_u}\quad\text{and}\tag{20}$$

$$R_3=\frac{N\overline{S_u^2}}{4\overline{T}_c}=\frac{\overline{S}_u\xi_u}{2}\tag{21}$$

Fig. 6 illustrates that $G_u(t)/t$ is defined as GATE frame rate, i.e., how many GATE frame intervals the system has in a time unit, which is equal to $1/\overline{T}_c$, as $t\to\infty$. What's more, when the system enters into a stable state, $G_u$equals $\overline{G}_u$ and T_c equals $\overline{T}_c$. Hence, R_4 can be given by:

$$R_4=\lim_{t\to\infty}\frac{1}{t}\sum_{i=1}^{G_u(t)}\frac{G_i^2}{2}=\lim_{t\to\infty}\frac{G_u(t)}{t}\frac{\sum_{i=1}^{G_u(t)}G_i^2}{2G_u(t)}=\frac{\overline{G_u^2}}{2\overline{T}_c}=\frac{\xi_u\overline{G_u^2}}{NS_u}\tag{22}$$

Since V_u, S_u and G_u are presented as a function of $\overline{T}_c$, we can have the following math formulas:

$$NV_u=(1-\rho_u-\xi_u-k_u)\overline{T}_c\tag{23}$$

$$(N/2)S_u=\xi_u\overline{T}_c\tag{24}$$

$$G_u=k_u\overline{T}_c\tag{25}$$

By substituting T_c from (20) in (23), (24), and (25), ξ_u and k_u can be rewritten as:

$$\xi_u=\frac{(N/2)S_u(1-\rho_u)}{NV_u+(N/2)S_u+G_u}\tag{26}$$

$$k_u=\frac{G_u(1-\rho_u)}{NV_u+(N/2)S_u+G_u}\tag{27}$$

Consequently T_c, R_2, R_3, and R_4 can be rewritten as:

$$T_c=\frac{NV_u+(N/2)S_u+G_u}{(1-\rho_u)}\tag{28}$$

$$R_2=\frac{(1-\rho_u-\xi_u-k_u)\overline{V}_u}{2}=\frac{NV_u^2(1-\rho_u)}{2(NV_u+(N/2)S_u+G_u)}\tag{29}$$

$$R_3=\frac{\overline{S}_u\xi_u}{2}=\frac{NS_u^2(1-\rho_u)}{4(NV_u+(N/2)S_u+G_u)}\tag{30}$$

$$R_4=\frac{\xi_u\overline{G_u^2}}{NS_u}=\frac{G_u^2(1-\rho_u)}{2(NV_u+(N/2)S_u+G_u)}\tag{31}$$

Finally, Lemma 1 can be proved by replacing R_1, R_2, R_3 and R_4 in (14) with (15), (29), (30), and (31).

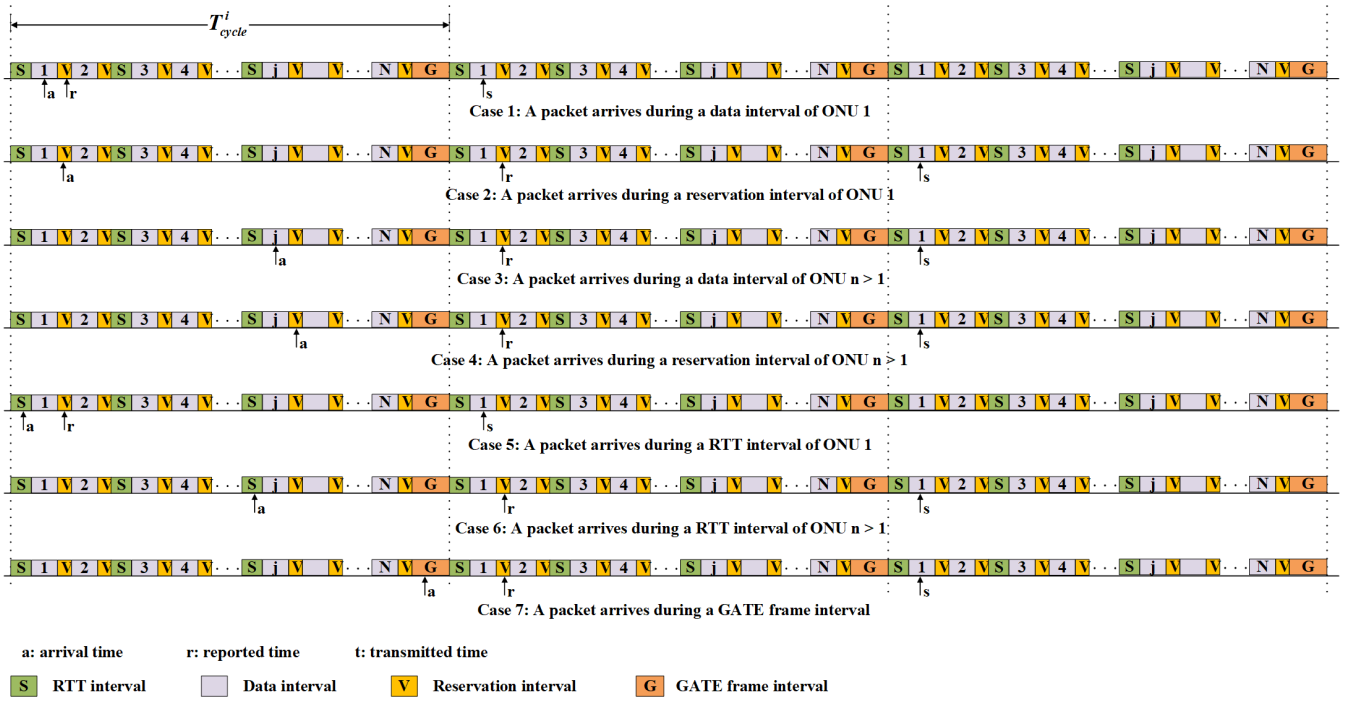

FIGURE 8. Possible scenarios of a packet arrival in US.

TABLE 3. Reservation-and-vacation time for US scheduling in PWC scheme.

Arrival during	Probability	Waiting time
Case 1: ONU_1's data	ρ_u/N	$NV_u + NS_u/2 + G_u$
Case 2: ONU_1's reservation	$(1-\rho_u-\xi_u-k_u)/N$	$2NV_u + NS_u + 2G_u$
Case 3: ONU_j's data	ρ_u/N	$(2N-j)V_u + \lfloor (2N-j+2)/2 \rfloor \cdot S_u + 2G_u$
Case 4: ONU_j's reservation	$(1-\rho_u-\xi_u-k_u)/N$	$(2N-j)V_u + \lfloor (2N-j+2)/2 \rfloor \cdot S_u + 2G_u$
Case 5: First RTT interval	$2\xi_u/N$	$NS_u/2 + NV_u + G_u$
Case 6: j^{th} RTT interval	$2\xi_u/N$	$2(N-j+1)V_u + (N-j+1)S_u + 2G_u$
Case 7: GATE interval	k_u	$NV_u + (N/2+1)S_u + G_u$

Lemma 2: The reservation-and-vacation time of US latency in PWC scheme can be defined as

$$\begin{aligned}\overline{Y}_u &= \frac{\rho_u(2NV_u + NS_u + 2G_u)}{2N} \\ &+ (1-\rho_u)(S_u + 2V_u) \\ &+ \left(1 - \frac{\left((N/2)S_u + G_u\right) \times (1-\rho_u)}{NV_u + (N/2)S_u + G_u}\right) \\ &\times \frac{(3N-2)(2N-2)V_u + 8(N-1)G_u + (3N^2-2N)S_u}{4N} \\ &+ \frac{(1-\rho_u)S_u\left((2V_u+S_u)\cdot\left(\frac{3N^2-6N}{8}\right) + (N-2)G_u\right)}{NV_u + (N/2)S_u + G_u} \\ &+ \frac{(1-\rho_u)G_u(2NV_u + (N+2)S_u + 2G_u)}{2\left(NV_u + (N/2)S_u + G_u\right)} \end{aligned} \tag{32}$$

Proof: The reservation-and-vacation delay is derived from the graphical argument, as shown in Fig. 8. $\overline{Y}_u$ depends on the probability for the ONU_1's data packet to arrive in a particular time interval and the extra time that this data packet must wait. Table 3 shows seven kinds of cases. From this table, we can compute $\overline{Y}_u$ as follows:

$$\begin{aligned}\overline{Y}_u &= \frac{\rho_u(2NV_u + NS_u + 2G_u)}{2N} \\ &+ \frac{(1-\rho_u-\xi_u-k_u)(2NV_u + NS_u + 2G_u)}{N} \\ &+ \sum_{j=2}^{N} \frac{\rho_u\left((2N-j)V_u + \left\lfloor\frac{2N-j+2}{2}\right\rfloor \cdot S_u + 2G_u\right)}{N} \\ &+ \sum_{j=2}^{N} \frac{\left((2N-j)V_u + \left\lfloor\frac{2N-j+2}{2}\right\rfloor \cdot S_u + 2G_u\right)}{N}\end{aligned}$$

$$\times (1-\rho_u-\xi_u-k_u) + \frac{\xi_u(2NV_u+NS_u+2G_u)}{N} + \sum_{j=2}^{N/2}\frac{2\xi_u(2(N-j+1)V_u+(N-j+1)\cdot S_u+2G_u)}{N} + \frac{k_u\,(2NV_u+(N+2)\,S_u+2G_u)}{2} \quad (33)$$

Hence, from this formula, (32) can be deduced, and Lemma 2 is proved.

Theorem 1: The mean US frame latency in the EPON system with pairwise-combination-based DBA scheme is expressed as follows:

$$\begin{aligned}\overline{D}_u &= \frac{\rho_u\overline{X_u^2}}{2\,(1-\rho_u)\,\overline{X}_u} + \frac{2NV_u^2+NS_u^2+2G_u^2}{4(NV_u+(N/2)S_u+G_u)} \\ &+ \frac{\rho_u(2NV_u+NS_u+2G_u)}{2N\,(1-\rho_u)} + (S_u+2V_u) \\ &+ \left(1-\frac{\left((N/2)\,S_u+G_u\right)\times(1-\rho_u)}{NV_u+(N/2)\,S_u+G_u}\right) \\ &\times \frac{(3N-2)(2N-2)V_u+8(N-1)G_u+(3N^2-2N)S_u}{4N\,(1-\rho_u)} \\ &+ \frac{S_u\left((2V_u+S_u)\cdot\left(\frac{3N^2-6N}{8}\right)+(N-2)\,G_u\right)}{NV_u+(N/2)\,S_u+G_u} \\ &+ \frac{G_u\,(2NV_u+(N+2)\,S_u+2G_u)}{2\left(NV_u+(N/2)\,S_u+G_u\right)} + \overline{X}_u+\overline{T}_{prop} \end{aligned} \quad (34)$$

Proof: In PWC-based DBA scheme, the mean US frame latency in the EPON system is obtained by adding the mean US queue delay, and the average frame service time to the average propagation delay, which is the data transmission time from the OLT to an ONU:

$$\overline{D}_u = \overline{W}_u + \overline{X}_u + \overline{T}_{prop} \quad (35)$$

By substituting (13) and (32) in (12), $\overline{W}_u$ is obtained. Then, replacing $\overline{W}_u$ in (35), Theorem 1 can be proved.

B. MEAN DS FRAME DELAY

For all we know, in the traditional EPON system, the DS frames are broadcast by the OLT. However, in PWC-based DBA scheme, the DS frames are buffered in the OLT with N DS queues and transmits DS frames in sync with the US transmissions.

In the downstream scheduling, each DS transmission window will consist of a DS data interval and a reservation interval. As shown in Fig. 9, the reservation interval is equal to guard time. Consequently, the reservation interval V_d is a constant value, which is equal to T_g.

Proposition 1: In our PWC-based DBA networks, the OLT-ONU distance is at least 10km. Hence, the DS transmission can be viewed as a scheduling system with exhaustive service.

Proof: As discussed in TW Grant policy, the shared TW T_{len} for the two combined ONUs is computed in the following equation:

$$T_{len}^{PWC} = \max\{B_{d1}+B_{d2}+T_g, RTT + B_{u1}+B_{u2}+2T_{msg}+T_g\} \quad (36)$$

The aim is to prove that in the PWC-based DBA networks, T_{len}^{PWC} is always equal to $RTT + B_{u1} + B_{u2} + 2T_{msg} + T_g$ in (35). According to [18], the DS transmission cycle length is dependent on DS transmission load, and the cycle length T_c^d can be computed as follows:

$$T_c^d = \frac{NV_d}{1-\rho_d} \quad (37)$$

In (36), we assume the PON system has 128 ONUs, and the reservation interval V_d is set to $1.512\mu s$, where the GATE frame service time is $0.512\mu s$ and the guard time is $1\mu s$. When the DS transmission load is 0.95, the T_c^d is calculated as $3.87ms$. Hence, every ONU has an average TW of $0.03ms$. Nevertheless, in PWC-based DBA networks, the OLT-ONU average distance is 10km, and the propagation time is about $0.05ms$. It also means RTT is $0.1ms$, and $RTT + B_{u1} + B_{u2} + 2T_{msg} + T_g > B_{d1} + B_{d2} + T_g$ is always true. Hence, T_{len}^{PWC} is always equal to $RTT + B_{u1} + B_{u2} + 2T_{msg} + T_g$. Consequently, in the DS traffic scheduling, the allocated bandwidth is much more than required. From another point of view, not only can the DS frames of an ONU at the OLT's buffer be transmitted but also the frame that arrived at the buffer during the transmission time.

Generally speaking, if US traffic load ρ_u is set to a given value, the cycle length can be computed and the DS upper bound delay can also be confirmed. From (28) and (37), the DS upper bound traffic load can be derived from $T_c^d = T_c$. Hence, the upper bound traffic load is expressed as:

$$\rho_d^{up} = 1 - \frac{(NV_d+G_d)\,(1-\rho_u)}{NV_u+(N/2)S_u+G_u} \quad (38)$$

As a result of the surplus bandwidth granted for the DS traffic, the transmission window in OLT allocated for an ONU is not always transmitting DS frames. In other words, DS timeslot is composed of not only the DS data intervals, reservation intervals, and the GATE frame intervals, but also the blank intervals, as shown in Fig. 9. The first and second moments of DS blank time are denoted by $\overline{S}_d$ and $\overline{S_d^2}$.

According to [20], the mean DS packet latency $\overline{W}_d$ is composed of three parts: the residual delay $\overline{R}_d$, the service delay $\overline{Q}_d$, and the reservation-and-vacation delay $\overline{Y}_d$. It can be written as:

$$\overline{W}_d = \overline{R}_d + \overline{Q_d} + \overline{Y}_d \quad (39)$$

where we have used the following definitions:

The residual delay $\overline{R}_d$ is equal to the residual time, which is the time that system needs to spend in finishing the on-going activity, for example: data interval, reservation intervals, the GATE frame intervals and the blank intervals.

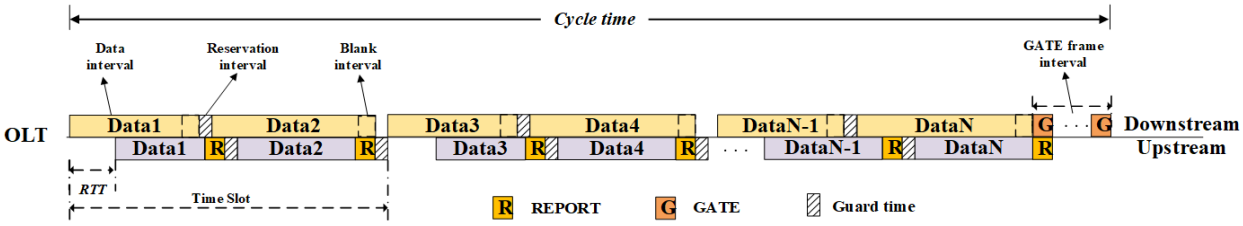

FIGURE 9. M/G/1 queueing model of DS scheduling.

The service delay $\overline{Q}_d$ is equal to the time for sending all the data packages to the ONU, and these packages arrived at the data buffer before this particular frame.

The reservation-and-vacation delay $\overline{Y}_d$ is equal to the total time of reservation intervals, the GATE frame intervals and the blank intervals.

According to Little's Theorem, the service delay $\overline{Q}_d$ can be expressed as follows:

$$\overline{Q}_d = \rho_d \overline{W}_d \tag{40}$$

Hence, $\overline{W}_d$ can be computed as:

$$\overline{W}_d = \overline{R}_d + \rho_d \times \overline{W_d} + \overline{Y}_d = \frac{1}{1-\rho_d}(\overline{R}_d + \overline{Y}_d) \tag{41}$$

Lemma 3: The residual delay $\overline{R}_d$ of DS traffic delay in PWC scheme can be defined as:

$$\overline{R}_d = \frac{\rho_d \overline{X_d^2}}{2\overline{X_d}} + \frac{\left(NV_d^2 + N\overline{S_d^2} + G_d^2\right)(1-\rho_d)}{2(NV_d + N\overline{S}_d + G_d)} \tag{42}$$

Proof: The analytical approach is similar to that in [21], and $\overline{R}_d$ can be written as:

$$\begin{aligned}\overline{R}_d &= \lim_{t\to\infty}\frac{1}{t}\int_0^t R(\tau)d\tau = R_1 + R_2 + R_3 + R_4 \\ &= \lim_{t\to\infty}\frac{1}{t}\sum_{i=1}^{X_d(t)}\frac{X_i^2}{2} + \lim_{t\to\infty}\frac{1}{t}\sum_{i=1}^{V_d(t)}\frac{V_i^2}{2} \\ &\quad + \lim_{t\to\infty}\frac{1}{t}\sum_{i=1}^{S_d(t)}\frac{S_i^2}{2} + \lim_{t\to\infty}\frac{1}{t}\sum_{i=1}^{G_d(t)}\frac{G_i^2}{2}\end{aligned} \tag{43}$$

where $X_d(t)$, $V_d(t)$, $S_d(t)$ and $G_d(t)$ are the numbers of data packets, reservation intervals, blank intervals and GATE intervals to time t, respectively. Moreover, X_i, V_i, S_i and G_i denote the time duration of the i^{th} data packet, reservation intervals, blank intervals and GATE intervals. In the limit as $t \to \infty$, $X_d(t)/t$ can be viewed as the average of the departure rate λ_d, and λ_d is equal to $\rho_d/\overline{X}_d$. Hence, R_1 can be computed as follows:

$$\begin{aligned}R_1 &= \lim_{t\to\infty}\frac{1}{t}\sum_{i=1}^{X_d(t)}\frac{X_i^2}{2} = \lim_{t\to\infty}\frac{X_d(t)}{t}\frac{\sum_{i=1}^{X_d(t)}X_i^2}{2X_d(t)} \\ &= \frac{\lambda_d\overline{X_d^2}}{2} = \frac{\rho_d\overline{X_d^2}}{2\overline{X_d}}\end{aligned} \tag{44}$$

Likewise, $V_d(t)/t$ can be viewed as the average of the reservation rate, which is equal to $(1-\rho_d-\xi_d-k_d)/\overline{V_d}$. ξ_d, k_d are the steady state probability of blank intervals and GATE frame intervals, respectively. Hence, R_2 can be given by:

$$\begin{aligned}R_2 &= \lim_{t\to\infty}\frac{1}{t}\sum_{i=1}^{V_d(t)}\frac{V_i^2}{2} = \lim_{t\to\infty}\frac{V_d(t)}{t}\frac{\sum_{i=1}^{V_d(t)}V_i^2}{2V_d(t)} \\ &= \frac{(1-\rho_d-\xi_d-k_d)\overline{V_d^2}}{2\overline{V}_d} = \frac{(1-\rho_d-\xi_d-k_d)\overline{V}_d}{2}\end{aligned} \tag{45}$$

$S_d(t)/t$ is defined as blank rate, i.e., how many blank intervals the system has in a time unit. In PWC scheme, every polling cycle only contains N blank intervals, when $t \to \infty$. Hence, we can write:

$$\frac{S_d(t)}{t} = \frac{\xi_d}{\overline{S}_d} \tag{46}$$

Consequently, R_3 becomes:

$$R_3 = \lim_{t\to\infty}\frac{1}{t}\sum_{i=1}^{S_d(t)}\frac{S_i^2}{2} = \lim_{t\to\infty}\frac{S_d(t)}{t}\frac{\sum_{i=1}^{S_d(t)}S_i^2}{2S_d(t)} = \frac{\overline{S_d^2}\xi_d}{2\overline{S}_d} \tag{47}$$

$G_d(t)/t$ is defined as GATE frame rate, i.e., how many GATE frame intervals the system has in a time unit, which is equal to $k_d/\overline{G_d}$, as $t \to \infty$. What's more, when the system enters into a stable state, G_d equals $\overline{G}_d$. Hence, R_4can be given by:

$$R_4 = \lim_{t\to\infty}\frac{1}{t}\sum_{i=1}^{G_d(t)}\frac{G_i^2}{2} = \lim_{t\to\infty}\frac{G_d(t)}{t}\frac{\sum_{i=1}^{G_d(t)}G_i^2}{2G_d(t)} = \frac{k_d\overline{G}_d}{2} \tag{48}$$

Following a similar approach discussed in the part of US delay analysis, ξ_d and k_d can be rewritten as:

$$\xi_d = \frac{N\overline{S}_d(1-\rho_d)}{NV_d + N\overline{S}_d + G_d} \tag{49}$$

$$k_d = \frac{G_d(1-\rho_d)}{NV_d + N\overline{S}_d + G_d} \tag{50}$$

Consequently R_2, R_3, and R_4 can be rewritten as:

$$R_2 = \frac{NV_d^2(1-\rho_d)}{2(NV_d + N\overline{S}_d + G_d)} \tag{51}$$

$$R_3 = \frac{N\overline{S_d^2}(1-\rho_d)}{2(NV_d + N\overline{S}_d + G_d)} \tag{52}$$

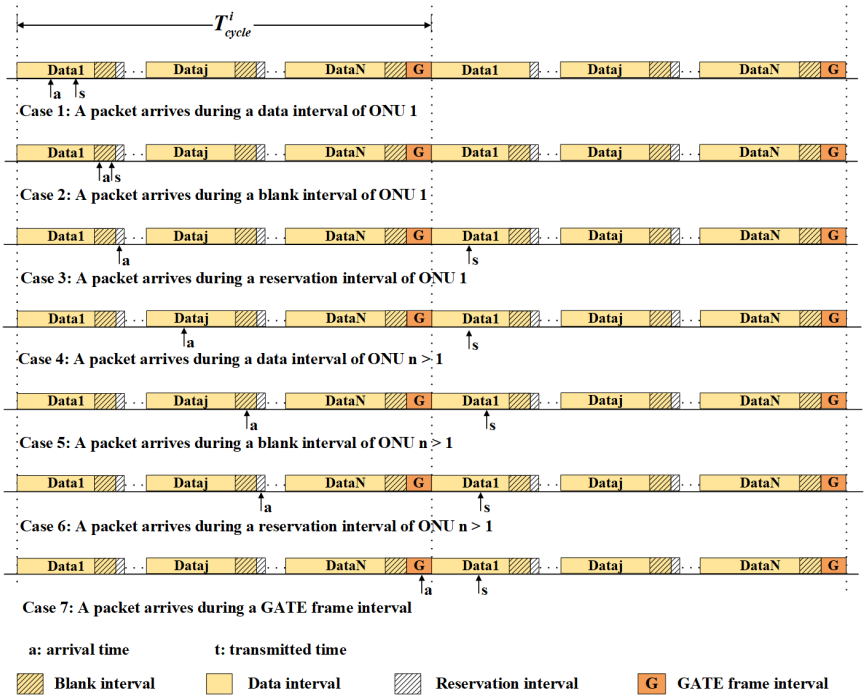

FIGURE 10. Possible scenarios of a packet arrival is DS.

TABLE 4. Reservation-and-vacation time for DS scheduling in PWC scheme.

Arrival during	Probability	Waiting time
Case 1: ONU$_1$'s data	ρ_d/N	0
Case 2: ONU$_1$'s blank	ξ_d/N	0
Case 3: ONU$_1$'s reservation	$(1-\rho_d-\xi_d-k_d)/N$	$(N-1)\left(V_d+\overline{S}_d\right)+G_d$
Case 4: ONU$_j$'s data	ρ_d/N	$(N-j+1)\left(V_d+\overline{S}_d\right)+G_d$
Case 5: ONU$_j$'s blank	ξ_d/N	$(N-j+1)V_d+(N-j)\overline{S}_d+G_d$
Case 6: ONU$_j$'s reservation	$(1-\rho_d-\xi_d-k_d)/N$	$(N-j)\left(V_d+\overline{S}_d\right)+G_d$
Case 7: GATE interval	k_d	0

$$R_4 = \frac{G_d^2(1-\rho_d)}{2(NV_d+N\overline{S}_d+G_d)} \tag{53}$$

Finally, Lemma 3 can be proved by replacing R_1, R_2, R_3 and R_4 in (43).

Lemma 4: The reservation-and-vacation time of DS latency in PWC scheme can be defined as:

$$\begin{aligned}\overline{Y}_d = &\frac{(1-\rho_d)NV_d\left(\frac{(N-1)}{2}\times\left(V_d+\overline{S}_d\right)+G_d\right)}{NV_d+N\overline{S}_d+G_d}\\ &+\frac{\rho_d\left(\frac{N(N-1)}{2}\times\left(V_d+\overline{S}_d\right)+(N-1)G_d\right)}{N}\\ &+\frac{\left(\frac{N(N-1)}{2}V_d+\frac{(N-1)(N-2)}{2}\overline{S}_d+(N-1)G_d\right)}{NV_d+N\overline{S}_d+G_d}\\ &\times(1-\rho_d)N\overline{S}_d\end{aligned} \tag{54}$$

Proof: The reservation-and-vacation delay is derived from the graphical argument, as shown in Fig. 10. $\overline{Y}_d$ depends on the probability for the ONU$_1$'s data packet to arrive in a particular time interval and the extra time that this data packet must wait. Table 4 shows seven kinds of cases. From this table, we can compute $\overline{Y}_d$ as follows:

$$\begin{aligned}\overline{Y}_d = &\frac{(1-\rho_d-\xi_d-k_d)\left((N-1)\times\left(V_d+\overline{S}_d\right)+G_d\right)}{N}\\ &+\sum_{j=2}^{N}\frac{\rho_d\left((N-j+1)\times\left(V_d+\overline{S}_d\right)+G_d\right)}{N}\\ &+\sum_{j=2}^{N}\frac{\xi_d\left((N-j+1)\times V_d+(N-j)\overline{S}_d+G_d\right)}{N}\end{aligned}$$

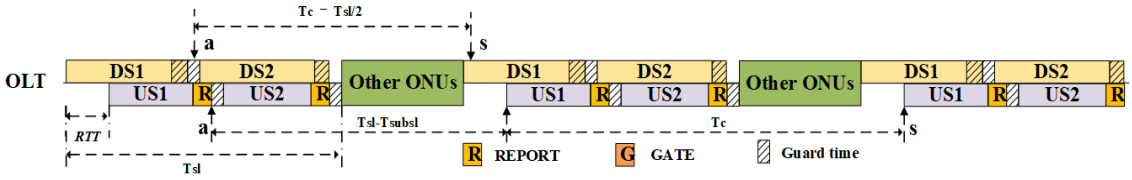

FIGURE 11. Illustration of upper bounds on US and DS frame delays in PWC scheme.

$$+\sum_{j=2}^{N}\frac{(1-\rho_d-\xi_d-k_d)((N-j)\times(V_d+\overline{S}_d)+G_d)}{N} \tag{55}$$

Hence, from this formula, (54) can be deduced, and Lemma 4 is proved.

Theorem 2: The mean DS frame latency in the EPON system with pairwise-combination-based DBA scheme is expressed as follows:

$$\begin{aligned}\overline{D}_d = &\frac{\rho_d\overline{X_d^2}}{2\overline{X_d}(1-\rho_d)}+\frac{\left(NV_d^2+N\overline{S_d^2}+G_d^2\right)}{2(NV_d+N\overline{S}_d+G_d)}\\&+\frac{NV_d\left(\frac{(N-1)}{2}\times\left(V_d+\overline{S}_d\right)+G_d\right)}{NV_d+N\overline{S}_d+G_d}\\&+\frac{\rho_d\left(\frac{N(N-1)}{2}\times\left(V_d+\overline{S}_d\right)+(N-1)\,G_d\right)}{N(1-\rho_d)}\\&+\frac{N\overline{S}_d\left(\frac{N(N-1)}{2}V_d+\frac{(N-1)(N-2)}{2}\overline{S}_d+(N-1)\,G_d\right)}{NV_d+N\overline{S}_d+G_d}\\&+\overline{X}_d+\overline{T}_{prop}\end{aligned} \tag{56}$$

Proof: In PWC-based DBA scheme, the mean DS frame latency in the EPON system is obtained by adding the mean DS queue delay, and the average frame service time to the average propagation delay, which is the data transmission time from the OLT to an ONU:

$$\overline{D}_d=\overline{W}_d+\overline{X}_d+\overline{T}_{prop} \tag{57}$$

By substituting (42) and (54) in (41), $\overline{W}_d$ is obtained. Then, replacing $\overline{W}_d$ in (57), Theorem 1 can be proved.

C. ESTIMATION OF US AND DS UPPER BOUND DELAY

As is illustrated in Fig. 11, the estimate of US and DS upper bound delay can be computed. What's more, the maximum frame service time of both US and DS frame is defined as $X_{\max}$.

Lemma 5: In PWC-based DBA scheme, the US upper bound latency in the EPON system is expressed as $2T_c - T_{msg} + T_{prop} + X_{\max}$.

Proof: If an US frame arrives at the ONU just after this ONU sends the REPORT frame to the OLT, this US frame will experience the maximum latency, as illustrated in Fig. 11. This US frame must wait to be reported to the OLT until the transmission window of REPORT frame in the next cycle. After being reported, this US frame has to wait a cycle. Hence, the total waiting time is $2T_c - T_{subsl}$, where the T_{subsl} is the ONU_1's transmission window and $T_{subsl} \geq T_{msg}$ is always true. The maximum frame service time of US frame $X_{\max} \geq X_u$. Therefore, the US upper bound delay $D_u^{\max}$ is given by:

$$\begin{aligned}D_u^{\max} &= 2T_c - T_{sl} + T_{prop} + X_{\max}\\&\leq 2T_c - T_{msg} + T_{prop} + X_{\max}\end{aligned} \tag{58}$$

Lemma 6: In PWC-based DBA scheme, the DS upper bound latency in the EPON system is expressed as $T_c - T_{msg} - (1/2)\,T_g + X_{\max}$.

Proof: If a DS frame arrives at the OLT buffer just when the DS transmission of the ONU is finished, this DS frame will experience the maximum latency, as illustrated in Fig. 11. This DS frame must wait to be transmitted to the ONU until the transmission window of the next cycle. Hence, the total waiting time is $T_c - (1/2)\,T_{sl}$, where the T_{sl} is the two combined ONUs' transmission window, and $T_{sl} \geq RTT + 2T_{msg} + T_g$ is always true. The maximum frame service time of DS frame $X_{\max} \geq X_d$. Therefore, the DS upper bound delay $D_d^{\max}$ is obtained as follow:

$$\begin{aligned}D_d^{\max} &= T_c - (1/2)\,T_{sl} + T_{prop} + X_{\max}\\&\leq T_c - T_{msg} - (1/2)\,T_g + X_{\max}\end{aligned} \tag{59}$$

V. SIMULATION MODEL AND RESULTS

This section gives out the performance evaluation and analyses of the proposed PWC-based DBA scheme. In order to fully highlight the advantages of the PWC-based DBA scheme over the traditional GS-based DBA scheme [9] in terms of the reduced packet latency and the saving-energy efficiency, we have conducted extensive numerical analyses using MATLAB platform.

A. CONSTANTS AND PARAMETERS

In the TDM-PON system, 1 OLT and N ONUs are assumed. The number of ONUs N, the length of RTT, and the length of guard time T_g are varied to analyze their impact on the performance of the proposed PWC-based DBA scheme. The US traffic load ρ_u and the DS traffic load ρ_d are varied from 0.05 to 0.95 [18]. According to MPCP protocol, the GATE frame's length is 64 bytes as well as the REPORT frame, corresponding to a transmission time being $0.512\mu s$. The mean frame servicing time $\overline{X}_u$ and $\overline{X}_d$ are both set to $5.09\mu s$, and the second moment $\overline{X_u^2}$ and $\overline{X_d^2}$ are equal to 51.44 $(\mu s)^2$ [9].

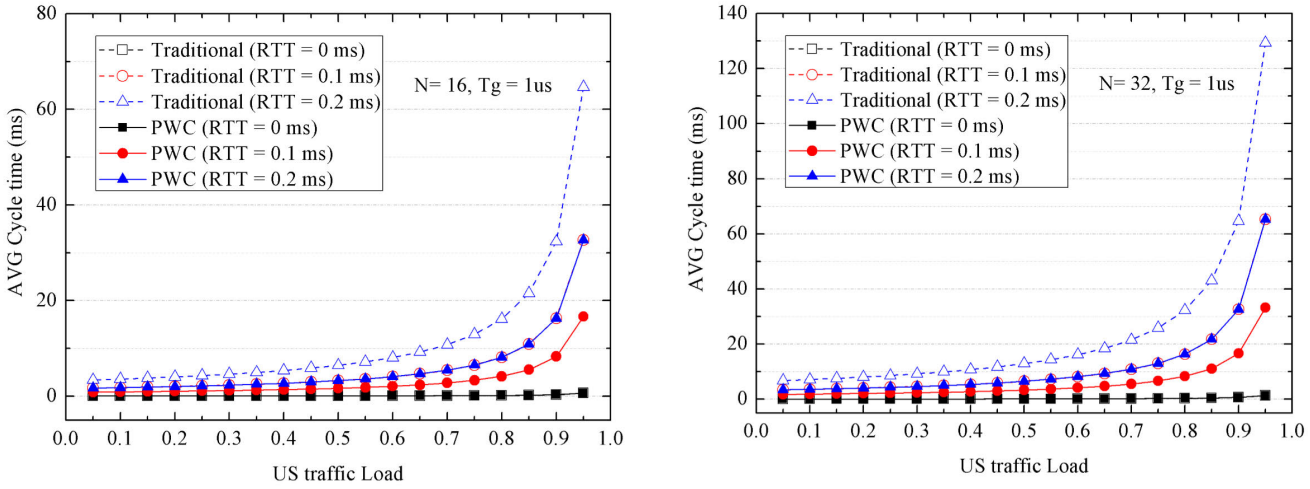

(a) *Tc vs.* ρ_u for various value of *RTT*(N=16). (b) *Tc vs.* ρ_u for various value of *RTT*(N=32).

FIGURE 12. Polling cycle time T_c as function of ρ_u and RTT.

In this scheme, the reservation interval $V_u = T_g + T_{msg}$, and $V_d = T_g$. The GATE frame interval time G is set to $7.2\mu s$ [18].

Since the OLT is always in active state and consumes the same energy all the time, we only consider the energy consumption of ONUs. We apply the sleep mode scheme on the ONU operation [3], [4]. For the sake of generality, the power consumption of the ONU's transceivers is represented by percentages in lieu of absolute values. P_{active} is viewed as the power consumption when both the RX and TX of the ONU are ON. P_{listen} is the power consumption of the ONU when RX is ON and the TX is OFF. Finally, the power consumption when both the RX and TX are OFF is defined as P_{sleep}. To obtain a realistic performance analysis, both US and DS traffic are generated by self-similar traffic modeling, and data are packed in standard Ethernet frames. In order to keep implementation simple, we assume that all ONUs have the same traffic parameters and loads.

The following part compares the performances of the existing GS- and PWC-based DBA schemes in terms of the following parameters: i) mean cycle-length, ii) upstream delay, iii) downstream delay, and iv) energy saving. In our simulations, we assume that all ONUs are put into a group, and hence the number of α is set to one. It is because that, based on the theoretical model presented in the section 4, the varied values of α have no effect on the above performance parameters. In the case, the OLT performs the US&DS bandwidth allocation by using the PWC method for each ONU, only after it collects all the REPORT messages from all the ONUs.

B. IMPACT ON CYCLE TIME

As given in (28), T_c is influenced by N, V_u, S_u, and ρ_u. Fig. 12 (a) shows the dependence of T_c on the RTT, and $N$is set to 16. In other words, it shows that S_u has a considerable effect on the length of cycle. Obviously, when ρ_u increases, T_c increases as well. What's more, a longer network reach greatly increases the value of T_c.

For the PWC-based DBA scheme, the average cycle-length is much shorter than that in the GS scheme. It is due to the fact that every polling cycle only contains $N/2$ *RTTs* in the PWC-based DBA scheme, while in the GS scheme, every cycle contains N *RTTs*. Consequently, the tradition GS scheme's cycle length is almost twice the cycle length of the PWC-based DBA scheme. As shown in Fig. 12(b), when N is set to 32, the *RTT*'s influence on the T_c is similar to Fig. 12(a). From these two pictures, we can draw a conclusion that a large number of ONUs considerably increases T_c.

Fig. 13(a) shows the dependence of T_c on the T_g, and N is set to 16. In other words, it shows that V_u has a considerable effect on the length of cycle. Obviously, a longer guard time greatly increases the value of T_c. As shown in Fig. 13(b), N is set to 32, and the $T_g's$ influence on the T_c is similar to Fig. 13(a).

C. IMPACT ON US FRAME DELAY

In this part, the US Frame Delay is studied in detail to detect these several parameters' influence on the D_u and $D_u^{\max}$. As shown in Fig. 14(a), when ρ_u increases, D_u increases as well. It is well to be reminded that the US mean delay is higher when the number of ONU increases.

Through comparison between the PWC scheme's results and the GS scheme's results, we can draw the conclusion that by adopting the proposed PWC method, the packet latency can be reduced effectively. The average US delay of the proposed scheme is much shorter than that of the GS-based scheme. It is because that the cycle length is compressed (see Fig. 13) by dynamically adjusting the polling sequence of the ONUs.

Fig. 14(b) shows the performance of US delay upper bound. Similarly, $D_u^{\max}$ increases for increasing ρ_u and N.

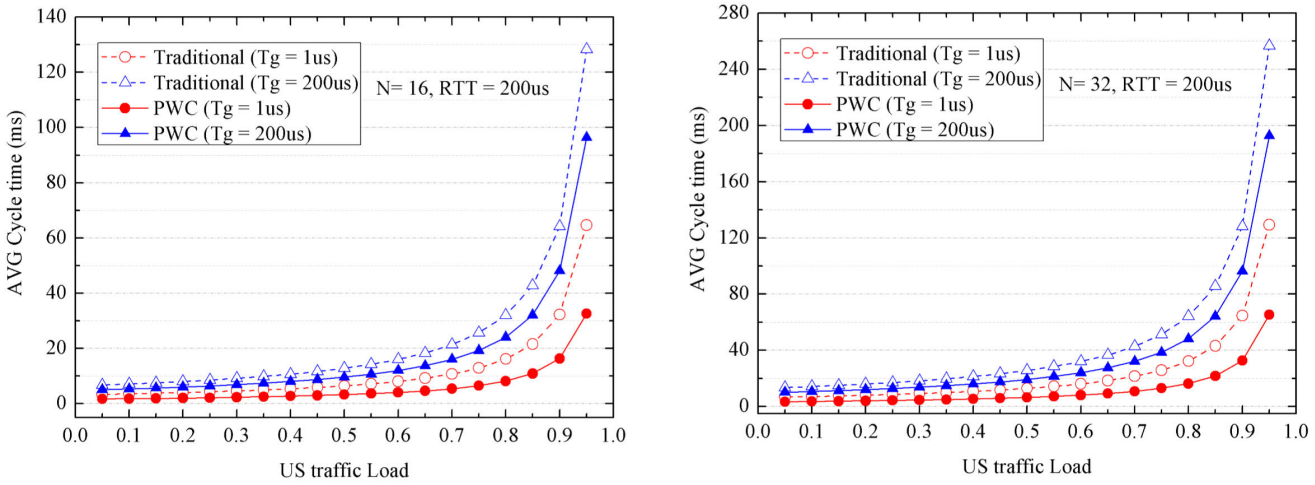

(a) *Tc vs.* ρ_u for various value of *Tg* (N=16). (b) *Tc vs.* ρ_u for various value of *Tg* (N=32).

FIGURE 13. Polling cycle time T_c as function of ρ_u and T_g.

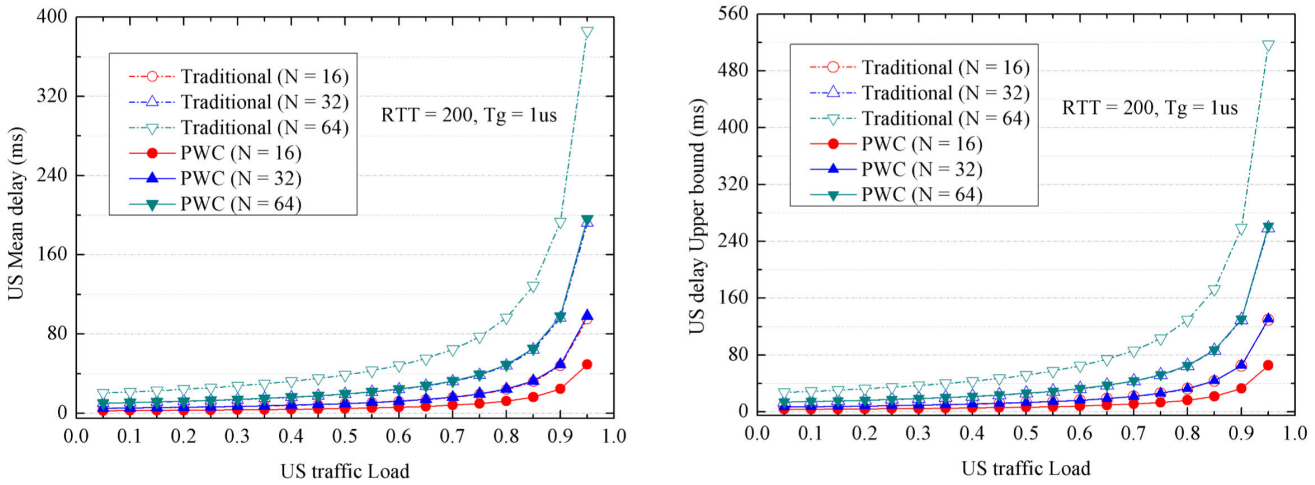

(a) Mean US delay *vs.* ρ_u. (b) US upper bound delay *vs.* ρ_u.

FIGURE 14. US frame delay ($\bar{D}u$ and D_u^{max}) as function of ρ_u.

From these two pictures, we can draw a conclusion that D_u is approximately three forth of $D_u^{\max}$. In addition, when the US traffic load is low, the US delay grows much more slowly. For example, when $\rho_u = 0.6$ and $N = 64$, the US mean delay of PWC-based DBA scheme is equal to $24ms$. However, when ρ_u increases to 0.85, the US mean delay increases to $65ms$.

Fig. 15 illuminates the dependence of D_u and $D_u^{\max}$ on the value of *RTT* given in (34) and (58). Obviously, the US delay is sensitive to the changing of *RTT*. Both D_u and $D_u^{\max}$ increase linearly with *RTT*. The reason is that a larger *RTT* lead to spending a longer time in transmitting data packets between the OLT and the ONUs. For example, when $RTT = 1$ms and $N = 64$, the corresponding D_u is about $120\,ms$. In addition, both D_u and $D_u^{\max}$ are positive correlation with the number of ONUs. A larger number of ONUs (i.e., a large EPON system) has a considerable effect on the US delay. In fact, one ONU can send or receive data packets again until the others finish their transmission and enter into sleep mode. Hence, as the number of ONUs in this system increases, every ONU must spend more time in waiting to transmit data packets at next cycle.

D. IMPACT ON DS LOAD UPPER BOUND

In the PWC-based DBA scheme, the transmission window is determined by the US required bandwidth, as mentioned above. Hence, $T_c > T_c^d$ is always true. Fig. 16 shows the DS load upper bound ρ_d^{up} versus US traffic load ρ_u given by (38). As shown in Fig. 16(a), even when *RTT* is set to 0 *ms* and

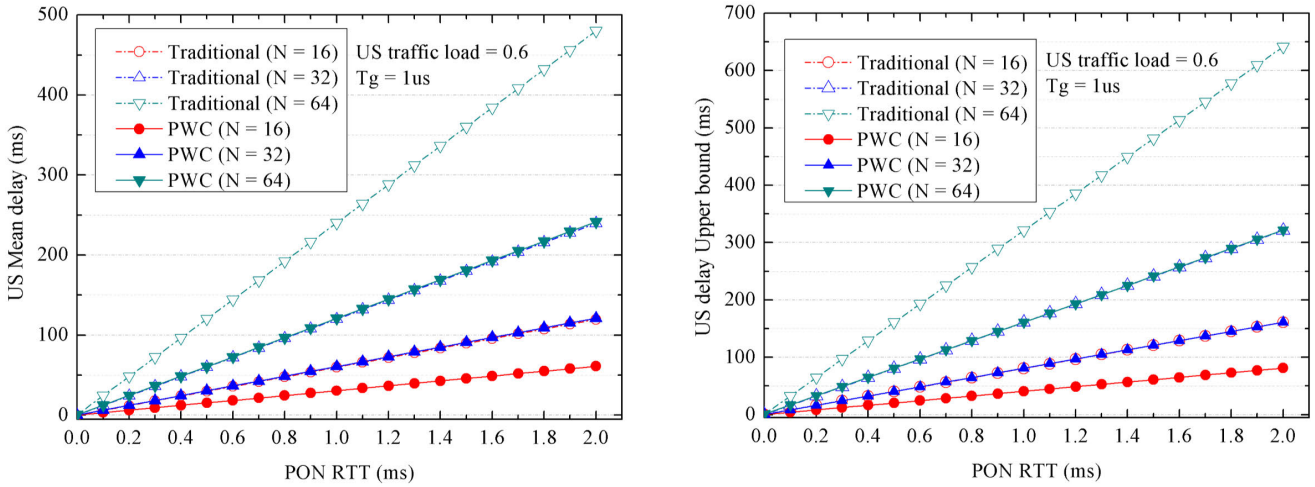

(a) Mean US delay *vs. RTT*.

(b) US upper bound delay *vs. RTT*.

FIGURE 15. US frame delay ($\bar{D}u$ and $D_u^{\max}$) as function of RTT for a given ρ_u.

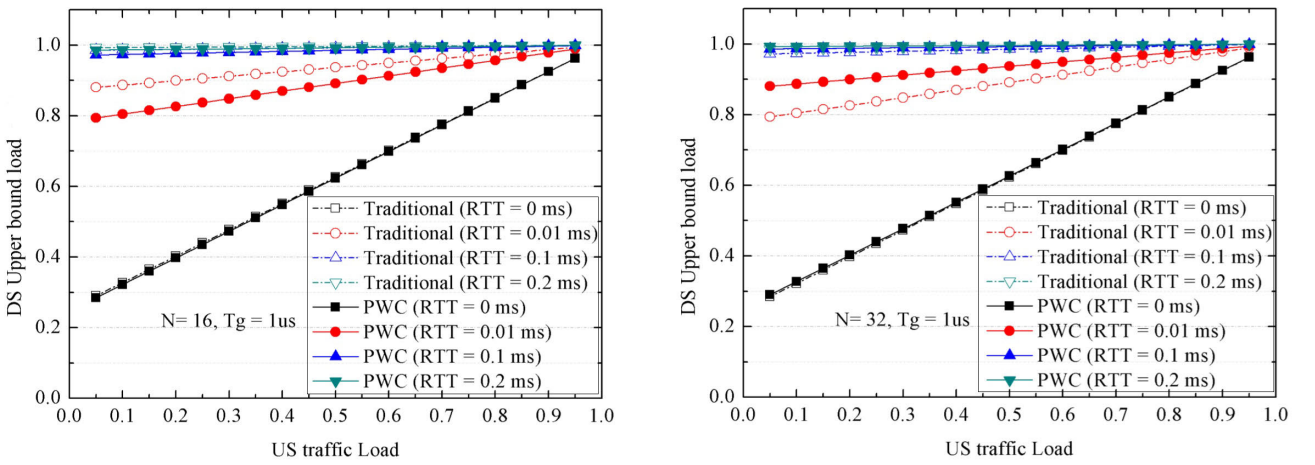

(a) DS upper bound traffic load vs. ρ_u various values of *RTT (N = 16)*.

(b) DS upper bound traffic load vs. ρ_u various values of *RTT (N = 32)*.

FIGURE 16. DS upper bound load vs. US traffic load.

the US traffic load is very low, the value of ρ_d^{up} is up to 0.3. For a given US traffic load, a longer network reach greatly increases the value of ρ_d^{up}. For instance, when *RTT* is set to $0.1ms$, the US upper bound load is always more than 0.95. Because RTT accounts for a large portion of T_{len}^{PWC} in light load condition, when RTT increases, TW is greatly enlarged and more DS data can be transmitted.

We can also see that the results in Fig. 16(a) look similar to that of Fig. 16(b). This means the number of ONU has little or no effect on ρ_d^{up}.

E. IMPACT ON DS FRAME DELAY

In order to study the DS delay performances, the results of the average DS delay and the maximum DS delay are shown in Fig. 17 and Fig. 18. As explained previously (see (56)), the D_d is the function of the DS traffic load ρ_d, while the $D_d^{\max}$ depends on cycle length, as shown in (59). What's more, the cycle length is a function of US traffic load ρ_u. Hence, this means that $D_d^{\max}$ is a function of ρ_u.

As shown in Fig. 17(a), when ρ_d increases, D_d increases as well. It is well to be reminded that the number of ONU has a negligible effect on D_d. Comparing Fig. 17(a) with Fig. 14(a), it shows US delay is much higher than the mean DS delay, when US traffic load is equal to the DS traffic load. For example, when $\rho_u = \rho_d = 0.6$ *ms*, D_u is $24ms$, and D_d is $10ms$. It is because in some cases (e.g. case 2, 3, 4, 6, 7) in Fig. 8, US data has to wait two polling cycles before it is transmitted, while DS data only need to wait at most one polling cycle (refer to Fig. 10). Fig. 17(b) shows the impact of US traffic load on the DS upper bound delay performance. From these two pictures, we can draw a conclusion that the D_d is approximately three forth of $D_d^{\max}$.

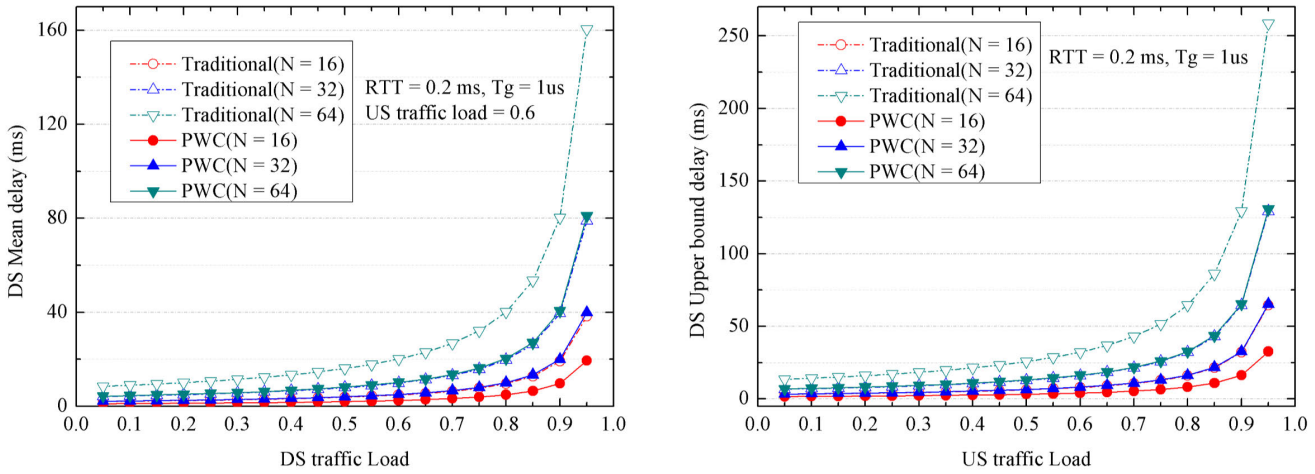

(a) Mean DS delay *vs.* ρ_d. (b) DS upper bound delay *vs.* ρ_u.

FIGURE 17. DS frame delay ($\bar{D}u$ and $D_u^{\max}$).

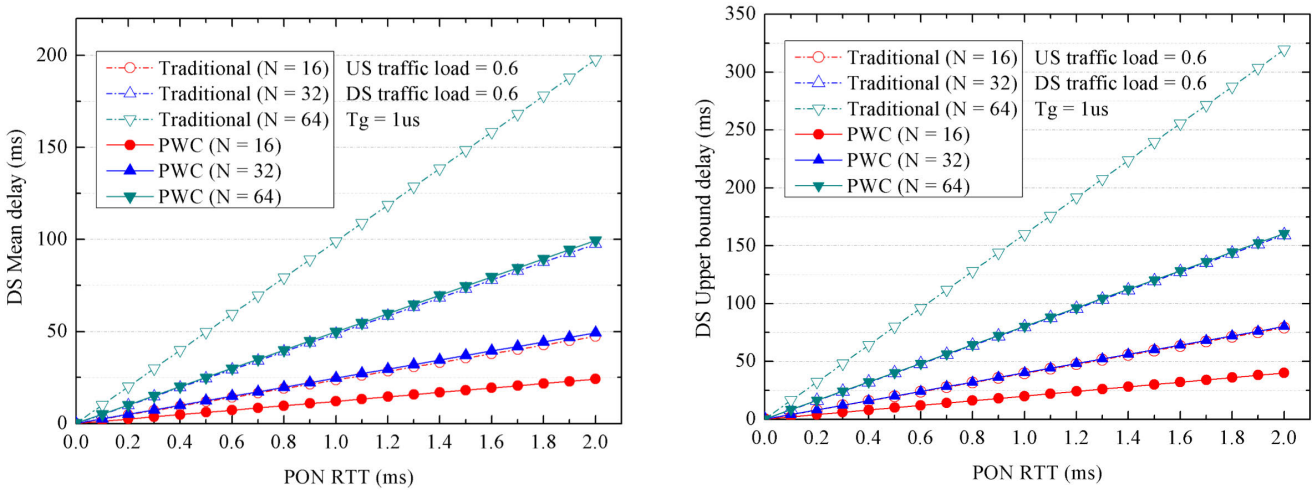

(a) Mean DS delay *vs. RTT*. (b) DS upper bound delay *vs. RTT*.

FIGURE 18. DS frame delay ($\bar{D}u$ and $D_u^{\max}$) vs. RTT.

Fig. 18 illuminates the dependence of D_d and $D_d^{\max}$ on the value of *RTT* given in (56) and (59). Obviously, the DS delay is sensitive to the different *RTT* values. Both D_d and $D_d^{\max}$ increase linearly with the *RTT*. In addition, both D_d and $D_d^{\max}$ are positive correlation with the number of ONUs. A larger number of ONUs have a considerable effect and change on the DS delay.

F. IMPACT ON ENERGY SAVING

For the PWC-based DBA scheme, the ONU has three different energy statuses, which correspond to active, listen and sleep states, respectively. What's more, the three different duration times are T_{active}^{PWC}, T_{listen}^{PWC} and T_{sleep}^{PWC}. For a given US traffic load, the cycle length can be calculated exactly and the value is a constant. From (6), we know that T_c^{PWC} is the sum of T_{active}^{PWC}, T_{listen}^{PWC}, and T_{sleep}^{PWC}. As illustrated in Fig. 3, T_{sleep}^{PWC} is dependent on T_c^{PWC}, and T_{sleep}^{PWC} is equal to $\left((N-1)/N\right) T_c^{PWC}$.

When T_{listen}^{PWC} is equal to $\left(1/N\right)\left(\rho_d^{up} - \rho_u\right) T_c^{PWC}$, T_{active}^{PWC} approaches the minimum value. Therefore, the maximum energy-saving efficiency can be obtained. When the time of listen mode is very short, for example, $T_{listen}^{PWC} = 0$, the energy-saving efficiency can be minimized.

Nevertheless, in the traditional GS scheme, the scheduling system only has two energy statuses. During the transmission window, the ONU is always in active mode, and the T_{active}^{GS} is equal to $\left(1/N\right) T_c^{GS}$. Outside the allocated TW of the ONU, it can be scheduled into the sleep state for saving energy, and the T_{sleep}^{GS} is equal to $\left((N-1)/N\right) T_c^{GS}$.

As depicted in Fig. 19, the PWC scheme outperforms the GS scheme, and the energy-saving efficiency η decreases as the US traffic load increases, which means that we can

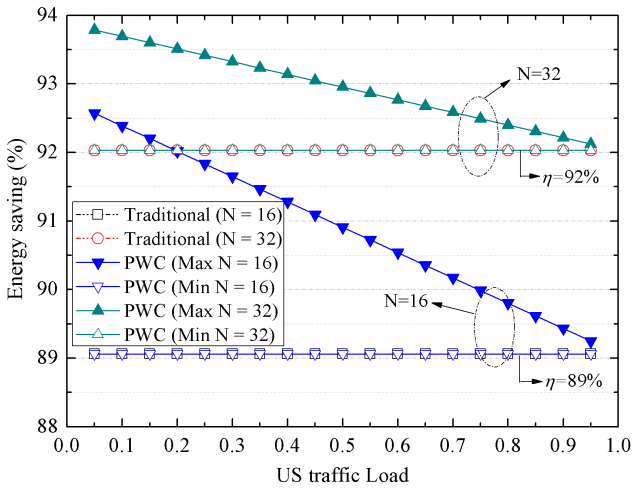

FIGURE 19. Energy saving efficiency η as function of US traffic load.

achieve higher energy efficiency when the system has a lower load. This is owing to almost every ONU's US bandwidth and DS bandwidth being granted with a very large value, in high-load region. In (1), the value of RTT is far less than $B_{d1} + B_{d2}$ or $B_{u1} + B_{u2}$, and RTT has minimal effect on the TW. Hence, in realistic EPON, the different propagation delays between OLT and ONU will only have minor effect on the ONU paring for our proposed PWC-based DBA scheme. It also means that the time of listen mode becomes shorter as US traffic load increases.

In general, both the energy saving efficiency and the latency performance in the TDM-PONs can be improved by adopting the proposed PWC-based DBA scheme, compared with the existing GS-based DBA scheme. These results demonstrate the superiority of the PWC-based DBA scheme.

VI. CONCLUSION

In this paper, we proposed and investigated a novel PWC-based DBA scheme for TDM-PONs, in case that both the US and DS transmission are considered, simultaneously. We pair any two ONUs in complementary ways so that the polling cycle length is compacted and latency is reduced. A comprehensive M/G/1 queuing analysis for the data latency performance was presented. Energy consumption of the proposed PWC-PON is reduced by the multiple-state energy-saving mode (i.e. active, listen and sleep states, compared with the two states: active and sleep states of GS-based scheme). Sufficient theoretical analysis and extensive simulation results demonstrate that the superiority of the PWC-based DBA scheme. From simulation results, we observe that the proposed PWC-PON can reduce US latency and DS latency by 50% compared with the existing GS-based DBA scheme. The energy saving efficiency is up to 3.5% higher than the benchmark when the US traffic load is light. Hence, compared with the existing GS-based DBA scheme, the proposed PWC-based DBA method does not only reduce the data packet latency by significantly compacting the cycle length, but also further improve the PON energy-saving efficiency by introducing the advanced sleep scheme. Our feature work will evaluate the performance of the PWC-PON policy in the context of 5G fronthaul.

REFERENCES

[1] C. Lange and A. Gladisch, "On the energy consumption of FTTH access networks," in *Proc. Opt. Fiber Commun. Conf. Nat. Fiber Optic Engineers Conf.*, San Diego, CA, USA, 2009, pp. 1–3.
[2] G. Kramer and G. Pesavento, "Ethernet passive optical network (EPON): Building a next-generation optical access network," *IEEE Commun. Mag.*, vol. 40, no. 2, pp. 66–73, Feb. 2002.
[3] R. Kubo, J. Kani, H. Ujikawa, T. Sakamoto, Y. Fujimoto, N. Yoshimoto, and H. Hadama, "Study and demonstration of sleep and adaptive link rate control mechanisms for energy efficient 10G-EPON," *IEEE/OSA J. Opt. Commun. Netw.*, vol. 2, no. 9, pp. 716–729, Sep. 2010.
[4] J. Zhang and N. Ansari, "Toward energy-efficient 1G-EPON and 10G-EPON with sleep-aware MAC control and scheduling," *IEEE Commun. Mag.*, vol. 49, no. 2, pp. S33–S38, Feb. 2011.
[5] H. Bang, J. Kim, S.-S. Lee, and C.-S. Park, "Determination of sleep period for cyclic sleep mode in XG-PON power management," *IEEE Commun. Lett.*, vol. 16, no. 1, pp. 98–100, Jan. 2012.
[6] R. O. C. Hirafuji, K. B. da Cunha, D. R. Campelo, A. R. Dhaini, and D. A. Khotimsky, "The watchful sleep mode: A new standard for energy efficiency in future access networks," *IEEE Commun. Mag.*, vol. 53, no. 8, pp. 150–157, Aug. 2015.
[7] Y. Yan, S.-W. Wong, L. Valcarenghi, S.-H. Yen, D. R. Campelo, S. Yamashita, L. Kazovsky, and L. Dittmann, "Energy management mechanism for Ethernet passive optical networks (EPONs)," in *Proc. IEEE Int. Conf. Commun.*, Cape Town, South Africa, May 2010, pp. 1–5.
[8] Y. Yan and L. Dittmann, "Energy efficiency in Ethernet passive optical networks (EPONs): Protocol design and performance evaluation," *J. Commun.*, vol. 6, no. 3, pp. 249–261, May 2011.
[9] D. P. Van, B. P. Rimal, M. Maier, and L. Valcarenghi, "ECO-FiWi: An energy conservation scheme for integrated fiber-wireless access networks," *IEEE Trans. Wireless Commun.*, vol. 15, no. 6, pp. 3979–3994, Jun. 2016.
[10] T. Berisa and M. Maier, "Low-latency polling for passive optical networks," *IEEE Commun. Lett.*, vol. 17, no. 6, pp. 1288–1291, Jun. 2013.
[11] A. Shao, Q. Dou, Y. Xiao, P. Chu, C. Zhu, Y. Peng, and K. Long, "Bandwidth allocation design to guarantee qos of differentiated services for a novel OFDMA-PON," in *Proc. 18th Asia–Pacific Conf. Commun. (APCC)*, Jeju Island, South Korea, Oct. 2012, pp. 775–780.
[12] T. D. Nguyen, T. Eido, and T. Atmaca, "An enhanced QoS-enabled dynamic bandwidth allocation mechanism for Ethernet PON," in *Proc. 1st Int. Conf. Emerg. Netw. Intell.*, Sliema, Malta, Oct. 2009, pp. 135–140.
[13] M. Bokhari and P. Saengudomlert, "Analysis of mean packet delay for upstream transmissions in passive optical networks with sleep mode," *Opt. Switching Netw.*, vol. 10, no. 3, pp. 195–210, Jul. 2013.
[14] H. Uzawa, K. Honda, H. Nakamura, Y. Hirano, K.-I. Nakura, S. Kozaki, and J. Terada, "Dynamic bandwidth allocation scheme for network-slicing-based TDM-PON toward the beyond-5G era," *J. Opt. Commun. Netw.*, vol. 12, no. 2, pp. A135–A143, 2020.
[15] S. Garg and A. Dixit, "Novel dynamic bandwidth and wavelength allocation algorithm for energy efficiency in TWDM-PON," in *Proc. 21st Int. Conf. Transparent Opt. Netw. (ICTON)*, Angers, France, Jul. 2019, pp. 1–4.
[16] P. Kourtessis, W. Lim, N. Merayo, Y.-M. Yang, and J. M. Senior, "Efficient T-CONT-Agnostic bandwidth and wavelength allocation for NG-PON2," *IEEE/OSA J. Opt. Commun. Netw.*, vol. 11, no. 7, pp. 383–396, Jul. 2019.
[17] M. Zhu, G. Li, S. Zhang, J. Gu, B. Chen, and Q. Sun, "Pairwise-combination-based DBA scheme for energy-efficient low-latency TDM-PONs," in *Proc. 10th Int. Conf. Adv. Infocomm Technol. (ICAIT)*, Stockholm, Sweden, Aug. 2018, pp. 128–132.
[18] G. Kramer, B. Mukherjee, and G. Pesavento, "IPACT a dynamic protocol for an Ethernet PON (EPON)," *IEEE Commun. Mag.*, vol. 40, no. 2, pp. 74–80, Feb. 2002.
[19] S. Bharati and P. Saengudomlert, "Simple derivation of mean packet delay for gated service in EPONs," in *Proc. 6th Int. Conf. Electr. Eng./Electron., Comput., Telecommun. Inf. Technol.*, Pattaya, Chonburi, May 2009, pp. 972–975.

[20] X. Bai, A. Shami, and Y. Ye, "Delay analysis of Ethernet passive optical networks with quasi-leaved polling and gated service scheme," in *Proc. 2nd Int. Conf. Access Netw. Workshops*, Ottawa, ON, Canada, 2007, pp. 1–8.
[21] S. Bharati and P. Saengudomlert, "Analysis of mean packet delay for dynamic bandwidth allocation algorithms in EPONs," in *J. Lightw. Technol.*, vol. 28, no. 23, pp. 3454–3462, Dec. 1, 2010.

MIN ZHU (Member, IEEE) is currently an Associate Professor and a Doctoral Supervisor with the National Mobile Communications Research Laboratory, Southeast University, Nanjing, China, and Purple Mountain Laboratories, Nanjing. He has published more than 50 articles in refereed journals and conferences of IEEE and OSA. His research interests include optical access networks and systems, network resource scheduling, and optimization algorithms. He also serves as an active reviewer for many international journals and conferences.

JIAHUA GU received the B.Sc. degree from the School of Electrical Engineering and Automation, Nanjing Normal University, Nanjing, China, in June 2016. He is currently pursuing the Ph.D. degree with the School of Information Science and Engineering, Southeast University, Nanjing. His research interests include C-RAN and machine learning.

GUIXIN LI received the M.S. degree from the School of Electronic Science and Engineering, Southeast University, Nanjing, China, in June 2019. He is currently with Huawei Technology Company, Ltd., Nanjing. His research interest includes passive optical networks.